



HAL
open science

Lossy compression of digital holograms using Gabor frames

Anas El Rhammad, Antonin Gilles, Patrick Gioia, Antoine Lagrange

► **To cite this version:**

Anas El Rhammad, Antonin Gilles, Patrick Gioia, Antoine Lagrange. Lossy compression of digital holograms using Gabor frames. Optics, Photonics and Digital Technologies for Imaging Applications VIII, Apr 2024, Strasbourg, France. pp.21, 10.1117/12.3017090 . hal-04661837

HAL Id: hal-04661837

<https://hal.science/hal-04661837v1>

Submitted on 25 Jul 2024

HAL is a multi-disciplinary open access archive for the deposit and dissemination of scientific research documents, whether they are published or not. The documents may come from teaching and research institutions in France or abroad, or from public or private research centers.

L'archive ouverte pluridisciplinaire **HAL**, est destinée au dépôt et à la diffusion de documents scientifiques de niveau recherche, publiés ou non, émanant des établissements d'enseignement et de recherche français ou étrangers, des laboratoires publics ou privés.

Lossy Compression of digital holograms using Gabor Frames

Anas El Rhammad^{1,*} Antonin Gilles¹ Patrick Gioia^{1,2} Antoine Lagrange¹

¹ IRT b<>com
Cesson-Sévigné
France

² Orange Labs
Cesson-Sevigne
France

Abstract

In this paper, we investigate the application of Gabor Frames (GFs) as an effective Time-Frequency (TF) analysis tool for compressing digital holograms. Our choice of GFs stems from their notable flexibility and accuracy in TF decomposition. Unlike some other techniques, GFs offer the advantage of accommodating both overcomplete and orthonormal signal representations. Furthermore, GFs have a robust mathematical foundation, opening doors to a broad spectrum of potential applications beyond compression. First, we provide an overview of essential concepts in GFs theory like dual GFs, analysis and synthesis operators. Second, we illustrate how GFs can be employed for digital holograms representation in the phase space domain. For compression purpose, we substitute the Short-Time Fourier Transform (STFT) used in the JPEG-PLENO Holography codec by tight GFs, and compare their encoding performance. We present and thoroughly discuss the rate-distortion graphs, shedding light on the efficacy of GFs in digital hologram lossy compression.

Keywords : Digital Holography, Time-Frequency Decomposition, Gabor Frames, Lossy Hologram Compression, JPEG-PLENO

1 Introduction

Due to its ability to capture and reconstruct three-dimensional (3D) scenes with high fidelity, Digital Holography (DH) has seen significant advancements across various applications: interferometry [1], microscopy [2], tomography [3], and 3D visualization [4]. In the latter application, DH stands out for its ability to provide all human visual system depth cues, without being affected by the accommodation-convergence conflict that occurs in most conventional 3D displays [5]. Thus, DH allows visualization with the naked eye and from a continuous set of viewpoints and depths, which render the user experience as realistic and comfortable as possible.

Although it possesses appealing characteristics for 3D interactive displays, the widespread use of DH is hindered by two main challenges [6]. The first one is related to the gigantic size of holographic data. Indeed, due to their diffractive nature, holograms are discretized at microscopic scale (order of magnitude of visible spectrum wavelength), which means that billions of pixels are required to record a high visual quality hologram with large dimension and field of view. Thus, despite the use of enormous storage and transmission resources, real-time processing of such huge quantity of raw data will be unreachable without effective compression techniques. The second major barrier concerns the non-stationary character of holographic signals, which further complicates the compression task. Unlike conventional images where high frequencies are less prominent and represent fine textures or edges, holograms spectrum presents much more high-frequency bands that contain main 3D information of the recorded scene. Therefore, applying traditional coding schemes (JPEG, MPEG...) to holographic data will omit the high frequencies resulting in a significant content degradation.

Over the past few years, multiple researches have been conducted to address the bottlenecks related to DH compression. Earlier attempts bypassed the challenging encoding of non-semantic holographic patterns by proposing an alternative scheme where the compression is performed on the initial 3D representation of the scene, followed by the hologram generation from decoded 3D data on the client side [7]. Although this technique achieves optimal coding efficiency thanks to powerful compression standards perfectly suited to the regular variation of 3D information in the source domain, it suffers from two major limitations : *i*) in most cases, the amplitude/phase or real/imaginary format of the hologram is provided instead of the 3D, multiview or RGB+depth information, *ii*) the computational charge imposed by the hologram generation requires substantial processing resources that may exceeds the client capabilities, thereby preventing real-time applications especially in case of holographic video and ultra-high resolution.

*This work has been achieved within the Research and Technology Institute b<>com, dedicated to digital technologies. It has been funded by the French government through the National Research Agency (ANR) Investment referenced ANR-A0-AIRT-07. Corresponding author: anas.elrhammad@b-com.com

In [8], the authors proposed another category of approaches that circumvents compression in the spatial domain of the hologram. These methods consist on propagating the hologram from its acquisition plane towards the object plane, and then encoding the obtained wavefield. When holograms have a large focusing depth or are captured from flat objects and with meticulous selection of the propagation distance, the refocused hologram exhibits sharpness akin to common images. This characteristic makes conventional image codecs highly effective in such scenarios. Although this approach allows notable compression gain [9], it is still constrained to microscopic holograms with nearly-flat scenes. Moreover, it necessitates a backward propagation for encoding and forward propagation for decoding, which may lead to heavy computational burden especially for scenes with wide depth range.

In order to expand the object-plane coding to deep scenes, a new coding paradigm based on Linear Canonical Transform (LCT) has been introduced in [10]. Indeed, the authors proposed a generalization of LCTs (including Fourier and Fresnel transforms) to model diffraction between arbitrary non-planar surfaces. Under some conditions related to surface shape, hologram pixel-pitch, and wavelength, they constructed an unitary transform that can be used to approximate the hologram at different distances of propagation. The obtained transform has been integrated in the default JPEG2000 codec using CDF 9/7 as sparsifying wavelets, achieving superior compression performance and well preservation of depth information and sharp details compared to the Fresnelet-based coding scheme [11, 12] and former JPEG2000 [13]. Despite the remarkable enhancement reached by this approach, its validity depends strongly on the geometry of the scene and on the precision of the depth profile approximation, making it unsuitable for multiple-object occluded scenes.

With all these limitations imposed by hologram’s 3D input and object plane coding methods, it seems that hologram plane compression is inevitable. Consequently, designing analysis routines specifically tailored to the irregular properties of holographic patterns is a main step towards an efficient and solid coding framework. The extensive research endeavors outcomes converged to a new compression scheme where the hologram is represented and encoded in an intermediate domain called *the Phase-Space* (*i.e.* the joint space of spatial coordinates and spatial frequencies). By adopting such representation, the intricate holographic fringes in the 2D spatial domain can be represented in a semantically meaningful way in the 4D phase-space domain, allowing to better interpret the 3D meaning of hologram features [14].

Phase-space analysis techniques have been used in several DH applications such as: accuracy and complexity enhancement of propagation operators such as the angular spectrum method [15], calculation acceleration of *Computed-Generated Holograms* (CGHs) [16, 17], depth estimation and diagnosis of distortions in DH through a visual interpretation of phase-space representations [18], motion compensation and segmentation of holograms with multiple occluded objects [19], symplectic formulation of light propagation on tilted reconstructions of CGHS [20] and digital holograms lossy compression [21, 22]. In the following, we only focus on the latter application. In [21], Gabor wavelets have been used as a TF analysis tool in order to decompose holographic patterns into a redundant set of diffracted light beams. Thanks to the optimal localization of Gabor wavelets in the TF domain with respect to the Heisenberg-Weyl uncertainty principle [23], the obtained phase-space expansion accurately represents the local directions of light emission. Unfortunately, such expansion is highly overcomplete and requires a time-consuming sparsification algorithm (e.g. Matching Pursuit) to achieve good compression rates. To avoid redundant transform, the authors of [22] proposed an alternative phase-space representation which deploys wave atoms. The latter form an orthonormal basis of directional wave packets and are particularly well suited for representing oscillatory signals. Although this approach produces sparse TF expansion suitable for compression, wave atoms suffer from sub-optimal localization in the phase-space.

The main goal of this paper is to explore the use of Gabor Frames (GFs) for lossy hologram compression. Unlike Gabor wavelets or wave atoms, GFs can be used in both overcomplete and orthonormal configuration. Additionally, they excel in minimizing cross-term interferences in phase-space and offers optimal TF localization. Our contribution involves studying the efficiency of tight GFs within the holographic compression framework of JPEG-PLENO [24]. The rest of the article is structured as follows: in Section 2, a brief overview of essential mathematical aspects in frames theory is provided. Then, Section 3 discuss the use of GFs for phase-space expansion of digital holograms. It also emphasizes how the JPEG-PLENO holography codec can be used for lossy compression using tight GFs transform instead of STFT. In Section 4, compression results obtained by tight GFs are compared to the former codec in terms of rate-distortion performance. Finally, Section 5 draws conclusions and proposes paths for future works.

2 Frames Theory

The notion of frame has been initially introduced in 1952 by *Richard Duffin* and *Albert Charles* in their pioneer paper [25] using non-harmonic Fourier series to determine the coefficients in a linear combination of vectors derived from a linearly dependent spanning set. This work laid the groundwork for understanding the essential requirements for a set of vectors to form a frame within a Hilbert space. In this section, an overview of frame theory is provided, focusing on key mathematical concepts and their relevance to signal processing. The review

begins by exploring the fundamental properties that define a frame, such as its existence condition, redundancy, and the role of the frame operator. These properties serve as the foundation for frame-based signal processing techniques. Following this, the complementary nature of the dual frame to the original frame is emphasized, which plays a crucial role in enabling the reconstruction of signals from their frame coefficients.

2.1 Mathematical properties of frames

The concept of bases in finite-dimensional spaces implies that the number of representative vectors is the same as the dimension of the space. When this number exceeds the dimension, it is still possible to have a representative set of vectors, except that they are linearly dependent, resulting in what is called a frame. Frames are redundant signal representation tools, placing fewer constraints compared to bases. Therefore, they are used to provide more flexibility in representing a signal.

- **Frame existence:**

Let consider a separable Hilbert space \mathcal{H} , a frame is a set of functions $\{\phi_j\}_{j \in J \subset \mathbb{Z}}$, such that there exist two strictly positive constants α and β , satisfying the following inequality:

$$\forall \psi \in \mathcal{H}, \quad \alpha \|\psi\|^2 \leq \sum_{j \in J} |\langle \psi, \phi_j \rangle|^2 \leq \beta \|\psi\|^2 \quad (1)$$

α and β represent the lower and upper bounds of the frame, respectively. They ensure a stable reconstruction of the function ψ . Furthermore, the smaller the difference between the bounds, the faster the numerical reconstruction.

When α and β are equal, the obtained frame is called *Tight Frame* and the vectors of the set $\{\phi_j\}_{j \in J}$ have the same norm. Another particular case is the *Parseval Frame* occurring when α and β are equal to 1. Such frame may be particularly useful in applications where the the signal energy must be preserved by the analysis operator (i.e. $\sum_{j \in J} |\langle \psi, \phi_j \rangle|^2 = \|\psi\|^2$).

- **Frame redundancy:**

For a N-dimensional Hilbert space \mathcal{H} , the redundancy of a frame $\{\phi_j\}_{j \in J \subset \mathbb{Z}}$ is defined by the ratio:

$$r = \frac{L}{N}, \quad (2)$$

where L represents the number of elements within the frame.

When $r > 1$, the frame is called *redundant* or *overcomplete*, which means it contains more elements than required to span the space \mathcal{H} . Such frame allows a more flexible and stable signal representation since its elements are linearly dependant. For $r = 1$, the frame is equivalent to a basis or tight frame, which ensures that every point in the signal space can be uniquely represented by a linear combination of frame vectors. A critical case is obtained for $r < 1$, where the frame is *undercomplete* and the signal cannot be perfectly retrieved from the frame elements.

While tight frames guarantee a minimalistic and unique representation, they are very efficient in terms of calculation load. On the other side, redundant frames can significantly enhance the versatility and robustness of signal representations, but, it also comes with increased computational complexity and storage requirements. Therefore, this trade-off should be considered when choosing an appropriate frame for a specific signal processing application.

- **Frame operator:**

A frame $\{\phi_j\}_{j \in J \subset \mathbb{Z}}$ can be can be represented using a linear operator \mathcal{F} defined by:

$$\mathcal{F} = \mathcal{S}\mathcal{A}, \quad (3)$$

where \mathcal{A} is the *analysis operator* given by:

$$\begin{aligned} \mathcal{A} : \mathcal{H} &\rightarrow \ell^2(J) \\ \psi &\mapsto \langle \psi, \phi_j \rangle, \end{aligned} \quad (4)$$

and \mathcal{S} is the *synthesis operator* given by:

$$\begin{aligned} \mathcal{S} : \ell^2(J) &\rightarrow \mathcal{H} \\ c &\mapsto \sum_{j \in J} c_j \phi_j. \end{aligned} \quad (5)$$

The analysis operator \mathcal{A} maps the signal ψ to a set of complex scalars $\{c_j = \langle \psi, \phi_j \rangle\}_{j \in J}$, called *frame coefficients*. If the frame is redundant ($r > 1$), these coefficients are not unique. The synthesis operator \mathcal{S} reconstruct the function ψ from a linear combination of coefficients $\{c_j\}_{j \in J}$ and the frame vectors $\{\langle \psi, \phi_j \rangle\}_{j \in J}$.

This reconstruction will be perfect in the case of tight frame, however, in the general case, it is mandatory to construct a dual frame in order to ensure a losslessly reconstruction (cf Section 2.2). The frame operator \mathcal{F} is linear, positive definite, self-adjoint, and invertible on \mathcal{H} . The existence condition of a frame (i.e. Eq 1) can thus be expressed in the following form:

$$\alpha\mathcal{I} \leq \mathcal{F} \leq \beta\mathcal{I}, \quad (6)$$

where \mathcal{I} is the identity operator.

2.2 Dual frames

Given that the frame operator is invertible, we obtain from Eq 6:

$$\frac{1}{\alpha}\mathcal{I} \leq \mathcal{F}^{-1} \leq \frac{1}{\beta}\mathcal{I}. \quad (7)$$

Thus, we deduce: if $\{\phi_j\}_{j \in J}$ is a frame with bounds α and β , the family of vectors $\{\{\tilde{\phi}_j\}_{j \in J}$ defined by:

$$\tilde{\phi}_j = (\mathcal{F}^{-1}\phi_j) \quad (8)$$

is called *dual frame*, where $\tilde{\alpha} = \alpha^{-1}$ and $\tilde{\beta} = \beta^{-1}$ are the lower and upper bounds, respectively.

In the general case, computing the dual frame may require iterative optimization algorithms leading to intensive computation charge and reconstruction errors in some scenarios. For the sake of simplicity, we will consider the painless case which stimulates that the dual frame can be obtained by simply inverting the diagonal of the matrix corresponding to the frame operator [26].

Given a frame $\{\phi_j\}_{j \in J}$ and its dual $\{\{\tilde{\phi}_j\}_{j \in J}$ in \mathcal{H} , any function $\psi \in \mathcal{H}$ can be expressed as:

$$\psi = \sum_{j \in J} \langle \psi, \tilde{\phi}_j \rangle \phi_j = \sum_{j \in J} \langle \psi, \phi_j \rangle \tilde{\phi}_j \quad (9)$$

This amounts to performing analysis using $\{\{\tilde{\phi}_j\}_{j \in J}$ and synthesis using $\{\phi_j\}_{j \in J}$, or vice-versa.

3 Proposed method

3.1 Gabor frames

GFs are a specific type of frames constructed by means of modulations and translations of a predefined function. GFs expansion corresponds to a discretized version of the continuous STFT transform. They serves as a powerful tool for phase-space representation, due to their optimal TF localization which enables an accurate analysis especially for signals with time-varying spectral content.

Let us consider a function $g \in \ell^2(\mathbb{C})$ and a pair of parameters $(a, b) \in \mathbb{R}^2$, a *Gabor system* G is the set of functions defined by:

$$G(s, a, b) = \{\mathcal{M}_{mb}\mathcal{T}_{na}g : (m, n) \in \mathbb{Z}^2\}, \quad (10)$$

where \mathcal{M} is the frequency modulation operator given by:

$$\mathcal{M}_w g(t) = g(t)e^{2i\pi wt}, \quad (11)$$

and \mathcal{T} is the translation operator given by:

$$\mathcal{T}_\tau g(t) = g(t - \tau). \quad (12)$$

G is the set of time-frequency shifting of the window g . The set of points $\Lambda_{a,b}$ discretizing the phase-space is called *lattice* and is defined as follow:

$$\Lambda_{a,b} = \{(na, mb) \mid (m, n) \in [1, \dots, M] \times [1, \dots, N]\}, \quad (13)$$

where N and M represent the number of translations and frequency modulations in the phase-space discretized grid, respectively .

If the functions in G satisfy the frame condition (i.e. Eq 1), then we speak of a Gabor frame defined by the operator $\mathcal{F}_{\Lambda_{a,b},g}$. The dual of a Gabor frame is also a Gabor frame defined on the same lattice and having the operator $\mathcal{F}_{\Lambda_{a,b},\tilde{g}}$, where \tilde{g} is the dual of g .

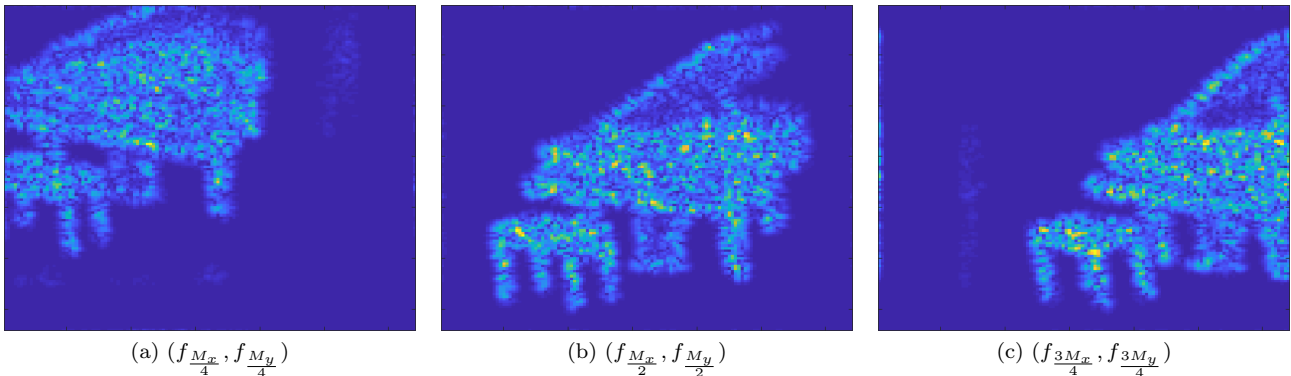


Figure 1: Amplitude distribution of reshuffled 4D GFs coefficients in phase-space for the ‘Piano4K’ hologram. The coefficients sub-blocks correspond to: (a) top left, (b) central and (c) bottom right frequency coordinates in the 4D space-frequency grid.

3.2 Hologram representation in phase-space using Gabor frames

Since the spatial frequency information of holograms is related to the diffraction angle via the grating equation [27], a good localization in both space and frequency domains would enable a precise extraction of the directions of light diffraction as well as their positions of emission. Thus, a better interpretation of the non-local features of holographic fringes involves a highly-localized expansion in the phase-space domain.

GFs are a promising candidate for an accurate and flexible phase-space representation of digital holograms, since they allow to break down the 2D non-stationary spatial components into well-localized chunks within the 4D space-frequency domain. The GFs expansion can be performed on regular or deformed lattice and its density can be controlled by tuning the sampling parameters of the defined lattice, which allows for a versatile representation in the phase-space. Moreover, GFs have the advantages to cover both orthonormal and overcomplete signal decomposition, depending on the targeted application.

To illustrate the utility of representing holograms in the joint space-frequency domain using GFs, let us consider a monochrome Computer Generated Hologram (CGH) having a resolution of 4096×4096 and representing a 3D scene of a Piano [28]. In order to achieve an optimal trade-off between space and frequency localization, a standard Gauss function will be considered for the GF’s window. The lattice $\Lambda_{a,b}$ is defined on a 4D regular grid where $a = (a_x, a_y) = (32, 32)$ and $b = (b_x, b_y) = a$.

Giving the separability of the window function and the frame operator on regular lattices, the GFs decomposition of 2D hologram can be computed by using a tensor product transform (i.e. 1D GFs expansion along hologram rows performed on lattice Λ_{a_x, b_x} followed by a second 1D expansion along columns and applied on lattice Λ_{a_y, b_y}). For a practical manipulation and visual interpretation of this representation, the resulting 4D coefficients are reorganized into a 2D matrix formed by sub-blocks placed next to each other. Indeed, each 2D sub-block in the spatial plane (n_x, n_y) regroups all the coefficients corresponding to a fixed spatial frequency (f_{m_x}, f_{m_y}) .

Fig. 1 shows the phase-space distribution of the GFs reorganized coefficients for the ‘Piano4K’ hologram. Contrary to spatial or Fourier distribution where the information would be completely spreaded-out, the phase-space representation using GFs is well-localized and reflects the 3D features of the recorded scene. Indeed, the amplitude of sub-blocks coefficients (Fig. 1a to Fig. 1c) constitutes the orthographic views of the piano. Thus, handling the hologram in the phase-space intermediate will pave the way for several functionalities such as : scalable representation, editing, motion compensation and efficient coding.

3.3 Proposed coding scheme

Our proposed holographic compression solution is mainly based on the INTERFERE compression scheme [29] proposed by VUB-imec as a response to the the Call for Proposal launched by JPEG-Pleno [30]. The INTERFERE codec supports two compression modes : *i*) *Mode I* is used for lossy compression of greyscale holograms, *ii*) *Mode II* is used for lossless compression of binary holograms. The main steps of the INTERFERE lossy encoder are listed below:

Tiling: The hologram may be decomposed into smaller tiles to reduce the computational cost, especially for high-resolution holograms. This allows a parallel encoding of tiles independently of each other.

Propagation: This step is optional and considered only for object plane coding. It consists of propagating the wavefield into a focused depth to enhance the compression performance.

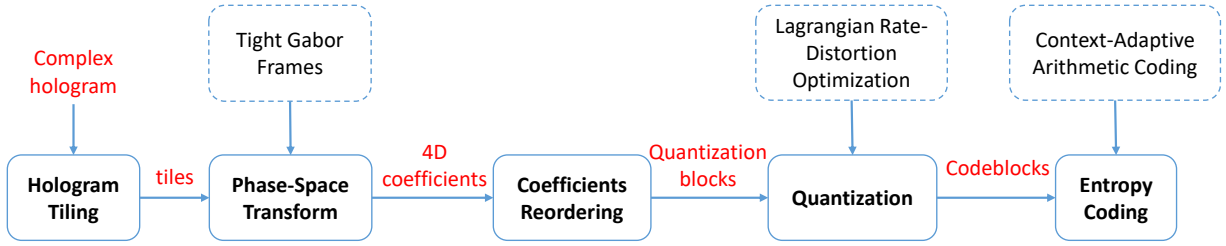


Figure 2: Overview of the modified INTERFERE lossy codec: the orthonormal STFT is replaced by TGFs.

Space-Frequency transform: Every (propagated) tile is subdivided into transform blocks (TBs), thus, controlling the space-frequency resolution. Every TB undergoes a discrete Fourier transform. This is equivalent to apply an orthonormal STFT using rectangular windows with zero overlap.

Quantization: Every TB is partitioned into quantization blocks (QBs), which regroups STFT coefficients from neighbouring spatial and frequency regions. The real and imaginary parts of each QB coefficients are quantized using a uniform scalar Mid-Rise Adaptive Quantizer. Then, a Rate-Distortion Optimization (RDO) module is applied on every quantized QB in order to determine the optimal candidate for quantization bit depth and range for a target distortion (i.e. SNR computed in the hologram plane). First, for every quantization bit depth per QB, an iterative method called *Golden-Section Search* is applied to determine the optimal quantization range values and its corresponding SNR. Then, an additional optimization layer using Lagrangian multiplier is performed for optimal bit depth allocation.

Entropy coding: The final step consists of losslessly encoding the quantization bit depth, ranges and complex coefficients. First, they are grouped, from neighbouring spatial and frequency regions, into CodeBlocks (CBs). Then, for each CB, an adaptive fixed-point arithmetic coding module is executed using one context for the quantization bit depth and zero context for the ranges and coefficients.

The obtained bitstream is decoded by applying inversely the same steps as the encoder. Thanks to the partitioning of coefficients into CBs, a 4D random access is possible by decoding independently each CB. This functionality is very useful for a quality or view-dependent scalable decoding of the compressed hologram.

The main contribution of this article concerns the space-frequency transform module in the INTERFERE encoder. Indeed, the STFT is replaced by a GFs transform to compute the 4D coefficients in phase-space. An overview of the modified INTERFERE encoder is shown in Fig. 2.

The efficiency of the INTERFERE codec rely heavily on the orthonormality of the STFT. Indeed, the calculation burden of the RDO module is drastically reduced, since it exploits the fact that for an orthogonal transform the overall L2 distortion induced by quantization can be written as the sum of individual L2 distortion resulted from each QB. In this way, the optimization routine is geniusly performed on much smaller blocks instead of entire hologram tile. The latter use case necessitates to compute inverse STFT to obtain distortion for every single quantization configuration.

In order to comply with this condition and allow a tractable RDO, a tight version of the GFs is utilized. Another advantage of using tight GFs (TGFs) is to avoid sparse representation algorithms such as matching or basis pursuit which are time-consuming. To further accelerate analysis for encoding and synthesis for decoding, a parallel implementation of the GFs expansion method described in the Large Time-Frequency Analysis Toolbox (LTFAT) [31] has been developed on GPU.

4 Experimental results

The proposed method was implemented in C++/CUDA on a PC system employing an Intel Core i9-9900X CPU operating at 3.50 GHz, a main memory of 32 GB and an operating system of Microsoft Windows 10 paired with a GPU NVIDIA GeForce RTX 2080Ti. The code was integrated in the INTERFERE software (version V3.02).

For hologram plane coding, the efficiency of compression schemes is evaluated by their ability to preserve the features of the complex hologram signal. Therefore, in all our experiments we use as quality metric the *Signal-to-Noise Ratio* (SNR) between the original hologram H_o and the compressed one H_c , defined by:

$$\text{SNR} = 10 \cdot \log_{10} \left(\frac{\sum_{i=1}^{L_x} \sum_{j=1}^{L_y} |H_o[i, j]|^2}{\sum_{i=1}^{L_x} \sum_{j=1}^{L_y} |H_o[i, j] - H_c[i, j]|^2} \right), \quad (14)$$

where (L_x, L_y) is the hologram resolution.

Hologram	Reconstruction Parameters			Phase-Space Expansion Resolution	
	Resolution	Aperture	Focus (cm)	STFT	TGF
'Piano16k'	16384 × 16384	4096 × 4096	1	512 × 512 × 32 × 32	128 × 128 × 128 × 128
'Dices16k'	16384 × 16384	4096 × 4096	1.31	512 × 512 × 32 × 32	128 × 128 × 128 × 128
'DeepDices2k'	2048 × 2048	2048 × 2048	0.74	256 × 256 × 8 × 8	64 × 64 × 32 × 32
'DeepCornellBox_16k'	16384 × 16384	4096 × 4096	25	512 × 512 × 32 × 32	128 × 128 × 128 × 128
'Astronaut'	2588 × 2588	1940 × 2588	17.2	256 × 256 × 11 × 11	64 × 64 × 44 × 44

Table 1: Reconstruction parameters and phase-space expansion resolution of the tested holograms.

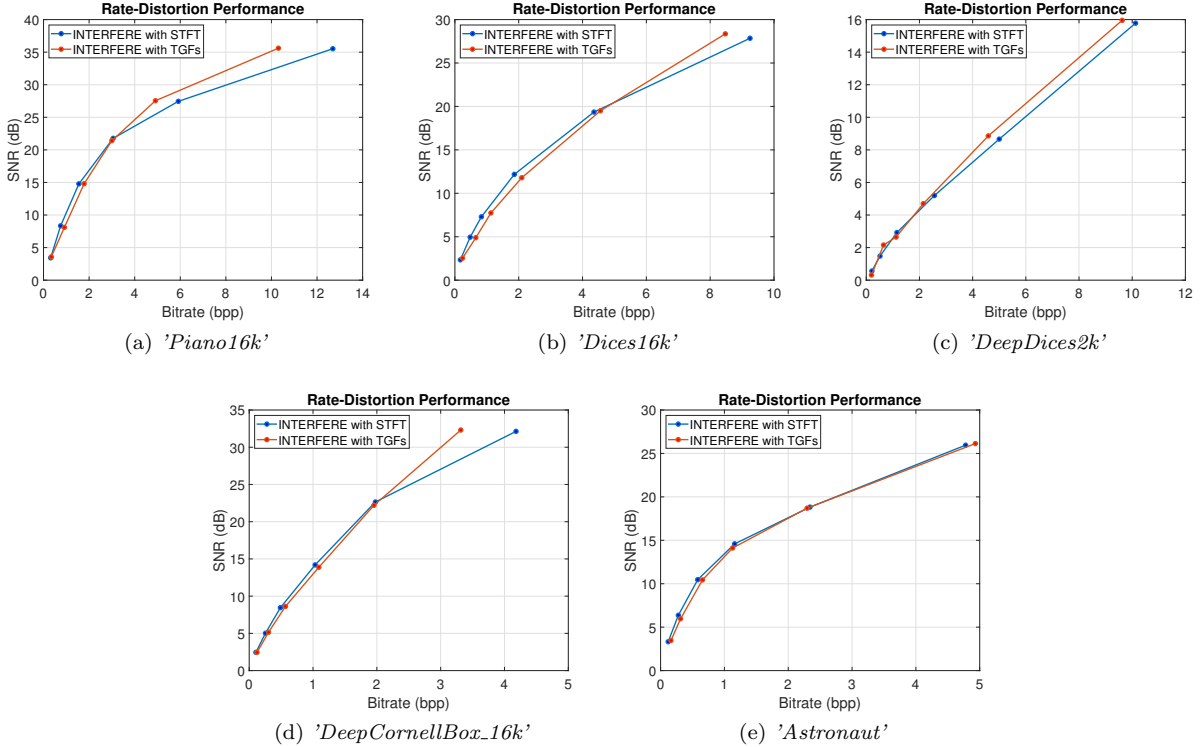


Figure 3: R-D graphs of the compressed hologram using STFT vs TGFs.

For color holograms, we consider the total rate needed to encode the R, G and B channels. The total distortion is computed as the mean value over the three color channels.

For the experiments, we considered 3 CGHs ('Dices16k', 'Piano16k' and 'DeepDices2k') taken from BCOM's database [28, 32], one CGH ('DeepCornellBox_16k') from INTERFERE-V's database [33], and one Optical Generated Hologram ('Astronaut') pertaining to HOLOGRAIL's database [8]. The reconstruction parameters (resolution, aperture size and focus distance) of the 5 holograms are listed in Table 1.

In order to objectively evaluate the effectiveness of the modified INTERFERE codec, we assessed the *Rate-Distortion* (R-D) performance obtained by compressing the hologram using TGFs as a phase-space transform and compare it to the one compressed by the default INTERFERE with STFT. The space-frequency resolution used for expanding each hologram is defined by the TBs size in case of STFT, whereas it is determined by the phase-space discretization parameters (M and N) in case of TGFs. Table 1 summarizes the spatio-frequency resolution for each tested hologram, which are manually tuned such as an near-optimal compression rate can be reached. Moreover, the QBs, CBs size and target SNRs used in RDO optimization are set to the default values defined in the common test conditions [34].

As depicted from the R-D graphs in Figure 3, the modified INTERFERE codec outperforms the former one in the high bitrate range, except for the 'Astronaut' hologram. For example, a compression gain of 1bpp and 0,87bpp is achieved for a target SNR value of 27.19dB and 32.13dB with respect to the 'Piano16k' and 'DeepCornellBox_16k' holograms, respectively. For the low bitrate range, using INTERFERE with STFT is slightly better compared to TGFs transform, except for the 'DeepDices2k' hologram which exhibits similar R-D performance.

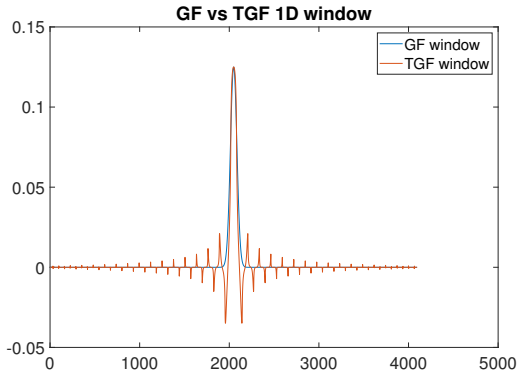


Figure 4: 1D GF’s vs TGF’s window ($M_x = N_x = 64$). TGF’s window presents vanishing oscillations around the Gaussian lobe.

For subjective evaluation, we visually compare the numerical reconstructions of the original holograms to the compressed ones at a fixed bitrate. As shown in Figure 5, the reconstruction of the ‘*Dices16k*’ hologram compressed ($\text{bpp} = 0.98$) by the modified INTERFERE codec is less distorted, especially on the top face of the green dice. For the compressed ($\text{bpp} = 1.25$) ‘*DeepDices2k*’ hologram, the visual quality of the reconstructed blue dice is clearly degraded when using STFT. This may be explained by the low spatial resolution of the space-frequency expansion. An other visual quality improvement is perceived on the reconstruction of the compressed ($\text{bpp} = 0.3$) ‘*Astronaut*’ hologram; indeed, the reconstruction obtained from the TGFs-based compression better retrieves the details present on the suits of the two astronauts standing in the background. Finally, the reconstructions of the decoded ‘*DeepCornellBox_16k*’ hologram present no visual differences between the modified INTERFERE codec and the default one at a compression bitrate of 1.06bpp.

Furthermore, we remark that all numerical reconstructions obtained from the modified version of the INTERFERE codec presents a slight aliasing-like (particularly visible around the blue dice’s dots and around astronaut’s silhouette). This may be caused by the vanishing oscillations around the Gauss lobe of the tight window used for analysis and synthesis, as illustrated in Figure 4.

In order to evaluate the efficiency of the proposed method in terms of computation time, we compare the encoding (including analysis, RDO and entropy coding) and decoding (including synthesis and entropy decoding) time of the modified and default INTERFERE codec. It turns out that these values are approximately equal for all the tested holograms. For example, the encoding and decoding time for the ‘*DeepCornellBox_16k*’ hologram is about 242s and 11s when using STFT, compared to 247s and 12s when utilizing TGFs, respectively.

5 Conclusion and Future Works

In this paper, we studied the use of GFs for lossy digital hologram compression. Giving their ability to accommodate both orthonormal and overcomplete expansion, optimal space-frequency localization and flexible signal expansion, GFs are considered as an efficacious tool for phase-space representation. In order to assess the effectiveness of GFs for encoding holographic signals, we modified the default version on the JPEG-PLENO holographic compression codec (INTERFERE) by replacing the orthonormal STFT with TGFs in the space-frequency transform module. The experimental results reveals that the modified INTERFERE codec outperforms the former one in the high bitrate range in terms of R-D performance. Moreover, subjective evaluation of numerical reconstructions shows a visual quality enhancement for TGFs-based compression. In addition, the complexity of the proposed method remains in the same range as the former INTERFERE codec.

In the future works, we plan to integrate the overcomplete GFs expansion configuration in the INTERFERE software and accordingly adapt the RDO module, in order to enable a better compression performance. Moreover, we foresee to extend the investigation to non-stationary GFs [35] to better deal with the non-regular character of holographic signals. Last but not least, the strong mathematical background of GFs theory opens a broad range of applications with respect to the symplectic transformations in the phase-space domain.

References

- [1] Kreis, T., [*Handbook of holographic interferometry: optical and digital methods*], John Wiley & Sons (2006).

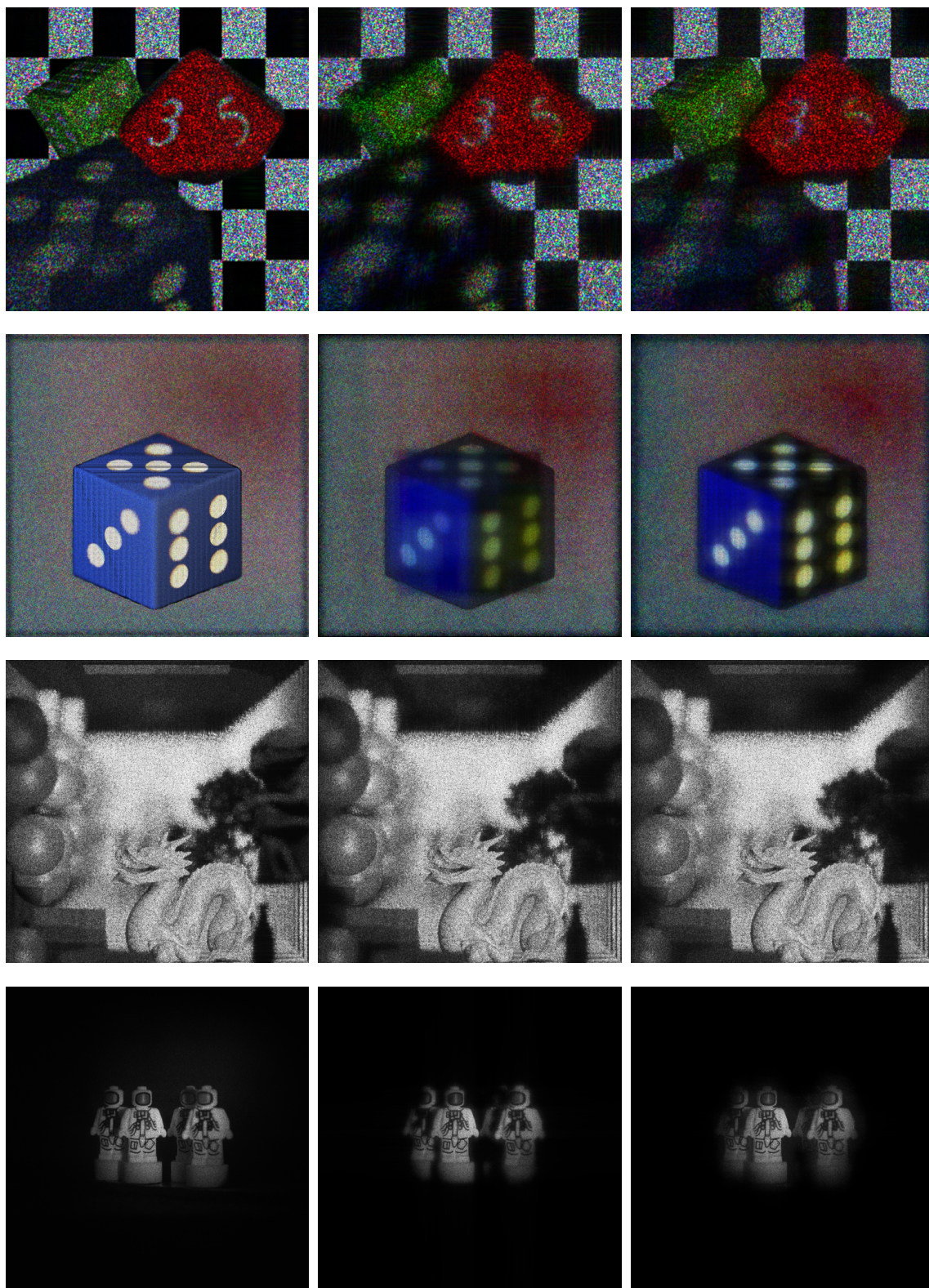


Figure 5: Numerical reconstructions of the original holograms (left column), and compressed hologram using INTERFERE with STFT (central column) and INTERFERE with TGFs (right column).

- [2] Kim, M. K., “Principles and techniques of digital holographic microscopy,” *SPIE reviews* **1**(1), 018005 (2010).
- [3] Charrière, F., Marian, A., Montfort, F., Kuehn, J., Colomb, T., Cuche, E., Marquet, P., and Depeursinge, C., “Cell refractive index tomography by digital holographic microscopy,” *Optics letters* **31**(2), 178–180 (2006).
- [4] Poon, T.-C., [*Digital holography and three-dimensional display: Principles and Applications*], Springer Science & Business Media (2006).
- [5] Lambooi, M. T., IJsselsteijn, W. A., and Heynderickx, I., “Visual discomfort in stereoscopic displays: a review,” *Stereoscopic Displays and Virtual Reality Systems XIV* **6490**, 183–195 (2007).
- [6] Blinder, D., Ahar, A., Bettens, S., Birnbaum, T., Symeonidou, A., Ottevaere, H., Schretter, C., and Schelkens, P., “Signal processing challenges for digital holographic video display systems,” *Signal Processing: Image Communication* **70**, 114–130 (2019).
- [7] Senoh, T., Wakunami, K., Ichihashi, Y., Sasaki, H., Oi, R., and Yamamoto, K., “Multiview image and depth map coding for holographic tv system,” *Optical Engineering* **53**(11), 112302–112302 (2014).
- [8] Bernardo, M. V., Fernandes, P., Arrifano, A., Antonini, M., Fonseca, E., Fiadeiro, P. T., Pinheiro, A. M., and Pereira, M., “Holographic representation: Hologram plane vs. object plane,” *Signal Processing: Image Communication* **68**, 193–206 (2018).
- [9] Bernardo, M. V., Pinheiro, A. M., and Pereira, M., “Benchmarking coding standards for digital holography represented on the object plane,” in [*Optics, Photonics, and Digital Technologies for Imaging Applications V*], **10679**, 123–132, SPIE (2018).
- [10] Blinder, D., Schretter, C., Ottevaere, H., Munteanu, A., and Schelkens, P., “Unitary transforms using time-frequency warping for digital holograms of deep scenes,” *IEEE Transactions on Computational Imaging* **4**(2), 206–218 (2018).
- [11] Liebling, M., Blu, T., and Unser, M., “Fresnelets: new multiresolution wavelet bases for digital holography,” *IEEE Transactions on image processing* **12**(1), 29–43 (2003).
- [12] Darakis, E. and Soraghan, J. J., “Use of fresnelets for phase-shifting digital hologram compression,” *IEEE transactions on image processing* **15**(12), 3804–3811 (2006).
- [13] Taubman, D. S., Marcellin, M. W., and Rabbani, M., “Jpeg2000: Image compression fundamentals, standards and practice,” *Journal of Electronic Imaging* **11**(2), 286–287 (2002).
- [14] Schelkens, P., Ebrahimi, T., Gilles, A., Gioia, P., Oh, K.-J., Pereira, F., Perra, C., and Pinheiro, A. M., “Jpeg pleno: Providing representation interoperability for holographic applications and devices,” *ETRI journal* **41**(1), 93–108 (2019).
- [15] Kozacki, T. and Falaggis, K., “Angular spectrum method with compact space–bandwidth: generalization and full-field accuracy,” *Applied Optics* **55**(19), 5014–5024 (2016).
- [16] Blinder, D. and Schelkens, P., “Accelerated computer generated holography using sparse bases in the stft domain,” *Optics express* **26**(2), 1461–1473 (2018).
- [17] Blinder, D., “Direct calculation of computer-generated holograms in sparse bases,” *Optics express* **27**(16), 23124–23137 (2019).
- [18] Birnbaum, T., Kozacki, T., and Schelkens, P., “Providing a visual understanding of holography through phase space representations,” *Applied Sciences* **10**(14), 4766 (2020).
- [19] Birnbaum, T., Blinder, D., Muhamad, R. K., Schretter, C., Symeonidou, A., and Schelkens, P., “Object-based digital hologram segmentation and motion compensation,” *Optics Express* **28**(8), 11861–11882 (2020).
- [20] Gioia, P., Gilles, A., Rhammad, A. E., and Vu-Ngoc, S., “Phase space formulation of light propagation on tilted planes,” (2024).
- [21] El Rhammad, A., Gioia, P., Gilles, A., Cagnazzo, M., and Pesquet-Popescu, B., “Color digital hologram compression based on matching pursuit,” *Applied optics* **57**(17), 4930–4942 (2018).

- [22] Birnbaum, T., Ahar, A., Blinder, D., Schretter, C., Kozacki, T., and Schelkens, P., “Wave atoms for digital hologram compression,” *Applied optics* **58**(22), 6193–6203 (2019).
- [23] Gröchenig, K., [*Foundations of time-frequency analysis*], Springer Science & Business Media (2013).
- [24] Schelkens, P., Gilles, A., Mahmoudpour, S., Oh, K.-J., Perra, C., and Pinheiro, A., “Standardization of holographic compression: Jpeg pleno,” in [*Digital Holography and Three-Dimensional Imaging*], HF1D–1, Optica Publishing Group (2020).
- [25] Duffin, R. J. and Schaeffer, A. C., “A class of nonharmonic fourier series,” *Transactions of the American Mathematical Society* **72**(2), 341–366 (1952).
- [26] Daubechies, I., Grossmann, A., and Meyer, Y., “Painless nonorthogonal expansions,” *Journal of Mathematical Physics* **27**(5), 1271–1283 (1986).
- [27] Goodman, J. W., [*Introduction to Fourier optics*], Roberts and Company publishers (2005).
- [28] Gilles, A., Gioia, P., Cozot, R., and Morin, L., “Hybrid approach for fast occlusion processing in computer-generated hologram calculation,” *Applied optics* **55**(20), 5459–5470 (2016).
- [29] Muhamad, R. K., Birnbaum, T., Blinder, D., Schretter, C., and Schelkens, P., “Interfere: A unified compression framework for digital holography,” in [*Digital Holography and Three-Dimensional Imaging*], Th4A–2, Optica Publishing Group (2022).
- [30] JTC1/SC29/WG1, S., “Final call for proposals on jpeg pleno holography,” 91st JPEG Meeting, (2021).
- [31] Søndergaard, P. L., “Efficient algorithms for the discrete gabor transform with a long fir window,” *Journal of Fourier Analysis and Applications* **18**, 456–470 (2012).
- [32] Gilles, A., Gioia, P., Cozot, R., and Morin, L., “Computer generated hologram from multiview-plus-depth data considering specular reflections,” in [*2016 IEEE International Conference on Multimedia & Expo Workshops (ICMEW)*], 1–6, IEEE (2016).
- [33] <http://erc-interfere.eu/downloads.html>.
- [34] Pinheiro, A. M., Prazeres, J., Gilles, A., Birnbaum, T., Muhamad, R. K., and Schelkens, P., “Definition of common test conditions for the new jpeg pleno holography standard,” in [*Optics, Photonics and Digital Technologies for Imaging Applications VII*], **12138**, 157–171, SPIE (2022).
- [35] Balazs, P., Dörfler, M., Jaillet, F., Holighaus, N., and Velasco, G., “Theory, implementation and applications of nonstationary gabor frames,” *Journal of computational and applied mathematics* **236**(6), 1481–1496 (2011).